

This article was downloaded by: [Siauliu University Library]

On: 17 February 2013, At: 06:47

Publisher: Taylor & Francis

Informa Ltd Registered in England and Wales Registered Number: 1072954 Registered office: Mortimer House, 37-41 Mortimer Street, London W1T 3JH, UK



## Advanced Composite Materials

Publication details, including instructions for authors and subscription information:

<http://www.tandfonline.com/loi/tacm20>

### Electrodeposition and mechanical properties of Ni-Al<sub>2</sub>O<sub>3</sub> nanocomposites

Jin-song Chen<sup>a</sup>, Bin Qiao<sup>a</sup> & Jian-ming Yang<sup>a</sup>

<sup>a</sup> College of Mechanical Engineering, Huaihai Institute of Technology, Lianyungang, 222005, China

Version of record first published: 10 Sep 2012.

To cite this article: Jin-song Chen, Bin Qiao & Jian-ming Yang (2012): Electrodeposition and mechanical properties of Ni-Al<sub>2</sub>O<sub>3</sub> nanocomposites, *Advanced Composite Materials*, 21:3, 233-240

To link to this article: <http://dx.doi.org/10.1080/09243046.2012.723361>

PLEASE SCROLL DOWN FOR ARTICLE

Full terms and conditions of use: <http://www.tandfonline.com/page/terms-and-conditions>

This article may be used for research, teaching, and private study purposes. Any substantial or systematic reproduction, redistribution, reselling, loan, sub-licensing, systematic supply, or distribution in any form to anyone is expressly forbidden.

The publisher does not give any warranty express or implied or make any representation that the contents will be complete or accurate or up to date. The accuracy of any instructions, formulae, and drug doses should be independently verified with primary sources. The publisher shall not be liable for any loss, actions, claims, proceedings, demand, or costs or damages whatsoever or howsoever caused arising directly or indirectly in connection with or arising out of the use of this material.

## Electrodeposition and mechanical properties of Ni–Al<sub>2</sub>O<sub>3</sub> nanocomposites

Jin-song Chen\*, Bin Qiao and Jian-ming Yang

*College of Mechanical Engineering, Huaihai Institute of Technology, Lianyungang 222005, China*

*(Received 18 March 2011; accepted 29 June 2012)*

The jet electrodeposition technology was used to prepare nano-Al<sub>2</sub>O<sub>3</sub> nanocomposites. Effect of the additive amount of nano-Al<sub>2</sub>O<sub>3</sub> particles and cathode current density on the nanoparticle content in composites was studied. The scanning electron microscope and X-ray diffractometer were adopted to analyze the micromorphology of the composites, research the effect of nanoparticle content in composites on the microhardness, bonding strength, and corrosion resistance. The results show that nickel deposited layer has the nanocrystalline microstructure, with the average grain size of about 40 nm; the content of nano-Al<sub>2</sub>O<sub>3</sub> particles in the deposited layer can reach 2.5 wt%; the composite coating prepared are all face-centered cubic structure and represent a (200) preferential orientation. With the increase of Al<sub>2</sub>O<sub>3</sub> content, the microhardness of coating will increase gradually and the bonding strength and corrosion resistance will first increase and then decrease.

**Keywords:** electrodeposition; nanocomposite; current density; bonding strength; corrosion resistance

### 1. Introduction

Electrodeposition of nanocomposite coatings, based on second phase hard particles dispersed in a metallic matrix, is gaining importance for potential engineering applications, however, the very low depositing rate of the conventional electrodeposition has limited the practical application of electrodeposition as a mean to prepare the composite materials [1,2].

Jet electrodeposition changes mass transfer process of deposition reaction by means of electrolyte high-speed flow on cathode surface, thus greatly increasing its limiting current density and enabling electrodeposition reaction to be performed continuously under very high current density, resulting in greatly refining crystalline grain in deposit layer and improving electrodeposition rate. The articles [3] reported that the deposit layer have crystalline microstructure. Till date, the Ni–Al<sub>2</sub>O<sub>3</sub> composite coatings fabricated by jet electrodeposition have not been reported.

In this present work, we prepared Ni–Al<sub>2</sub>O<sub>3</sub> nanocomposite coatings by jet electrodeposition technology. The effect of the concentration of Al<sub>2</sub>O<sub>3</sub> in the electrolyte and cathode current density on the amount of Al<sub>2</sub>O<sub>3</sub> codeposited in the composites was systematically studied. Microhardness and bonding strength and corrosion resistance of the Ni–Al<sub>2</sub>O<sub>3</sub> nanocomposites were also investigated.

---

\*Corresponding author. Email: jinsong20001@163.com

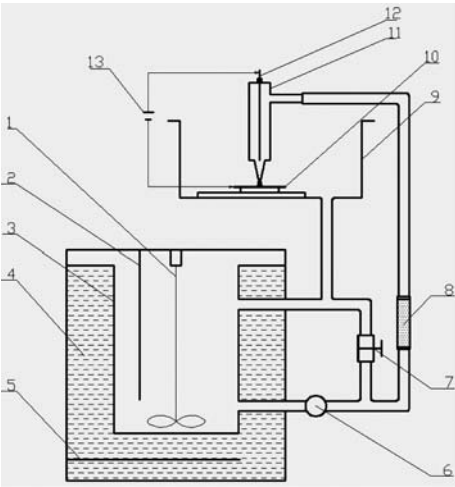


Figure 1. Diagram of jet electrodeposition equipments. (1) agitator (2) temperature transducer (3) vessel with electrolyte (4) distilled water (5) heater (6) centrifugal pump (7) valve (8) flowmeter (9) electrodepositing room (10) cathode (11) nozzle (12) anode and (13) current power.

2. Experimental details

2.1. Experimental equipments

The schematic representation of jet electrodeposit equipments are shown in Figure 1. The electrolyte was pumped from the vessel with invariable temperature electrolyte, and then reflowed to the vessel from the output of electrodeposting room via the bump of filter, and the flowmeter. The electrolyte temperature was measured by the heater and temperature transducer. The jet speed was adjusted by flowmeter.

During the jet electrodeposition process, the electrolyte is jetted on a cathode surface directly because of the existence of electric field between the cathode and anode located in the jet nozzle, as the electric current travels along the jet stream to the cathode, the deposition takes place only on the local cathode surface area where the jet impinges on. Thus, jet electrodeposition provide high depositing rate. In addition, the grain size refining effect of jet electrodeposition is more efficient.

2.2. Composition of electrolyte and processing parameters

The electrolyte used was based on a standard nickel Watt solution. The composition and processing parameters are given in Table 1.  $\text{Al}_2\text{O}_3$  particles with a mean diameter of 50 nm were used. Each electrolyte was mixed by magnetic stirring for 24 h, and subsequently by ultrasonic agitation for 30 min just prior to electrodeposition. Electrodeposition was carried out on vertical electrodes, and the electrolyte was agitated during electrodeposition with a magnetic stirrer.

Table 1. Composition of the electrolyte and processing parameters.

Composition of electrolyte	Processing parameter
$\text{NiSO}_4 \cdot 6\text{H}_2\text{O}/250 \text{ g L}^{-1}$	pH/4.0
$\text{NiCl}_2 \cdot 6\text{H}_2\text{O}/60 \text{ g L}^{-1}$	Temperature of electrolyte/50 °C
$\text{H}_3\text{BO}_3/40 \text{ g L}^{-1}$	Electrodepositing time/20 min
Additive/0.2 g L <sup>-1</sup>	Jet speed of electrolyte/1 m·s <sup>-1</sup>

### 2.3. Composition and properties analysis

The surface morphology and the components of the deposits were studied by using a field emission scanning electron microscope (FESEM, LEO-1530VP) with energy dispersive analyzer system (EDX). The weight fraction of aluminum was determined by using the aluminum to oxygen ratio 2:3 determined by the chemical formula  $\text{Al}_2\text{O}_3$ . The phase constitution of the deposits was characterized via X-ray diffraction (XRD). It was carried out by powder diffraction method at room temperature using a D/MAXRC X-ray diffractometer.

Vickers microhardness tests were conducted on an HXS-1000A microhardness tester using a load of 50 g applied for 10 s. Each hardness value was an average of five measurements.

The bonding strengthened between the composite and substrate was measured on SANSI-028A type universal tensile machine under the following conditions: loading speed 1.0 mm/min and load 0.1 KN. Specimens first, with the diameter of 20 mm and thickness of 100  $\mu\text{m}$  on the low-carbon steel substrate was prepared, then jointed to another piece of low-carbon steel with inorganic glue. Finally, the test was carried out after full solidification.

The corrosion behavior of composite coatings was evaluated by weight-loss method in a 4% HCl solution, which is given by equation as  $V = \Delta W / s \cdot t$ , where  $V$  is the corrosion rate;  $\Delta W$  is lose weight;  $s$  is exposed surface area in the corrosive liquid; and  $t$  is the corrosion time. Specimens with area of  $30 \times 20$  mm were prepared. The mass of the change of the specimens was measured by the analytical balance with precision of 0.1 mg. Before weighing, the specimens were cleaned by ultrasonic cleaning machine.

## 3. Result and discussion

### 3.1. Composition of nanocomposites

Figure 2 represents that wt% of  $\text{Al}_2\text{O}_3$  in the composite varies with different contents (10–40 g/L) of  $\text{Al}_2\text{O}_3$  particles in the electrolyte. The result shows that the incorporation of nanoparticles has a proportional relation with the content of particles suspended in the electrolyte. This phenomenon can be explained that, the more particulates in suspension within electrolyte, the more particulates travel to around the cathode surface through stirring and the more ones embedded in metal matrix, resulting an increase in the incorporation of  $\text{Al}_2\text{O}_3$ .

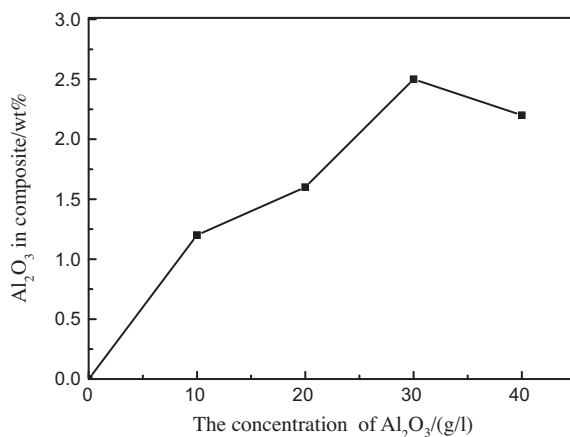


Figure 2. Effect of concentration on the wt% of  $\text{Al}_2\text{O}_3$  in the composite coatings.

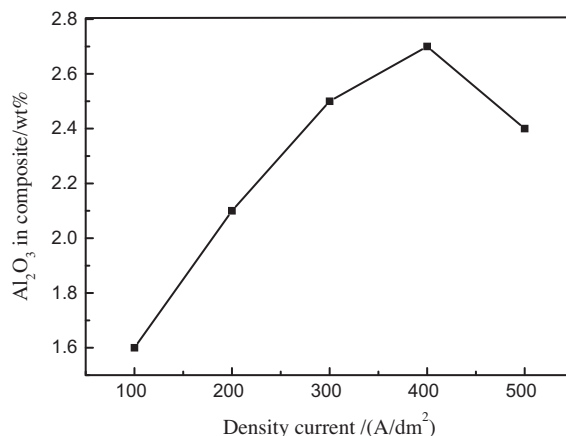


Figure 3. Effect of current density on the wt% of Al<sub>2</sub>O<sub>3</sub> in the composite coatings.

However, when the content of Al<sub>2</sub>O<sub>3</sub> in electrolyte surpassed 30 g/L, the Al<sub>2</sub>O<sub>3</sub> wt% began to decrease. It can be attributed that, on the one hand, the metal matrix has not been able to take so many adsorbed particulates at this point any more, and on the other hand, particulates themselves, due to colliding each other in electrolyte, are agglomerated and result in the decrease of degree of charge at particle surface.

Another reason may be related to those surplus particles dispersed in electrolyte, which scour and seep away the ones not fully embedded on the cathode. Therefore, the particles should not be excessively added into electrolyte and a proper addition of strengthening particle is essential [4,5].

Figure 3 represents that wt% of Al<sub>2</sub>O<sub>3</sub> in the composite varies with cathode current density (100–500 A/dm<sup>2</sup>). It is found that, when the Al<sub>2</sub>O<sub>3</sub> particle in the electrolyte is added to certain amount, the current density of Al<sub>2</sub>O<sub>3</sub> particle content in the coating will increase first and then decrease. This is because, with the increase of cathode current density, the cathode over potential will increase accordingly, the electric field force increases, the electrostatic attraction of nanoparticles with positive ion increases, playing a certain role in the codeposition of particle and matrix metal. However, when the cathode current density is too high, the deposition velocity of matrix metal is enhanced and the particle is transported near the cathode and the velocity of embedding into coating is slower than the metal deposition velocity, which will also lead to the decrease of Al<sub>2</sub>O<sub>3</sub> particle content in the coating. In addition, the particles embedded into the cathode surface cover parts of cathode surface. What's more, the particle conductivity is so poor that the actual area of the cathode decreases, leading to the increase of actual current density and causing a lot of hydrogen. It will also prevent the codeposition of particle and matrix metal [6,7].

### 3.2. Microstructure analysis

The scanning electron microscope of surface morphologies of Ni–Al<sub>2</sub>O<sub>3</sub> nanocomposites is represented in Figure 4. It is observed that the texture of pure nickel coating is uneven. With the increase of nano-Al<sub>2</sub>O<sub>3</sub> content, the density and smoothness of coating will be improved significantly. The reason for this situation is that small nano-Al<sub>2</sub>O<sub>3</sub> particles suspended in electrolyte play a certain role in nucleation objectively, increasing the number of growing nuclear, refining the grain of deposition, restraining the growth of nucleation grain, and making the metal deposition layer relatively compact and smooth [8,9]. The measured grain size

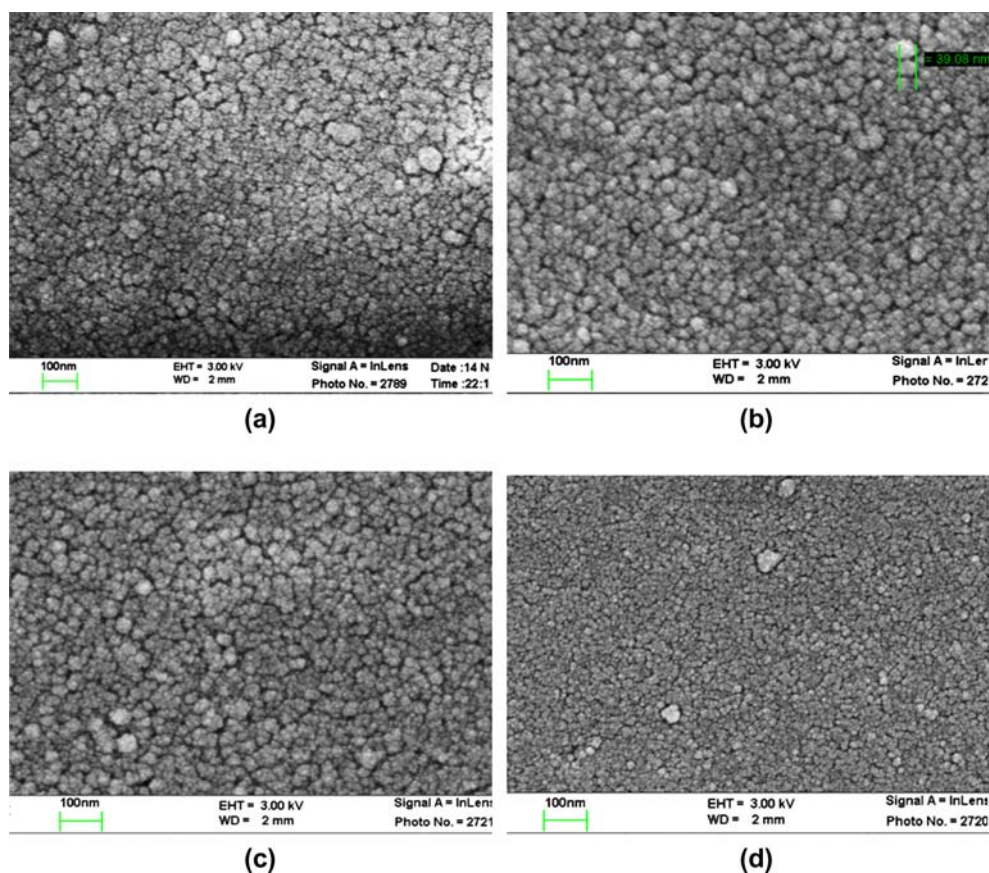


Figure 4. Microstructures of composites, (a) pure nickel (b) 1.2 wt%  $\text{Al}_2\text{O}_3$  (c) 1.6 wt%  $\text{Al}_2\text{O}_3$  and (d) 2.5 wt%  $\text{Al}_2\text{O}_3$ .

of coating texture in Figure 4(b) is about 40 nm. Although, the nano- $\text{Al}_2\text{O}_3$  distribution condition in coating cannot be clearly distinguished, it can be identified that Ni- $\text{Al}_2\text{O}_3$  composite deposition layer has 'double nanostructure,' i.e. the sizes of base metal grain and additive grain are all within the nanorange. This is because the high current density of jet electrodeposition enhances the cathode overpotential directly, decreases the critical crystal nucleus radius of nucleation, increases the nucleation number, restrains the epitaxial growth trend of grain, and avoids the production of bulky grain and refines the grain, making the jet electrodeposition technology to obtain nanocrystalline coating in the DC condition directly.

The XRD patterns and preferential orientation of the several specimens indicate changes in texture of such coatings which are dependent on the  $\text{Al}_2\text{O}_3$  content of the coatings (Figure 5). It can be found that the crystal planes corresponding to each diffraction peak are (111), (200), and (220) in turn. Both specimens are face-centered cubic structure and represent a (200) preferential orientation. With the increase in the  $\text{Al}_2\text{O}_3$  content of the composites, the orientation index of (111) decrease and that of (200) increase. A change in preferred orientation would lead to the difference between the coatings; it is possible that the disturbing of the particles affects the growth of crystallites which leads to the evolution of surface diffraction density and orientation and orientation.

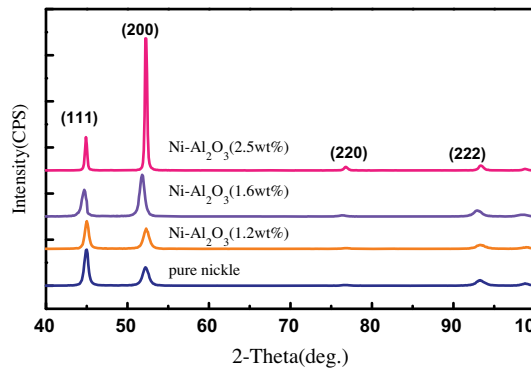


Figure 5. X-ray patterns of composite.

### 3.3. Microhardness

Figure 6 shows the relationship between Al<sub>2</sub>O<sub>3</sub> content and coating microhardness. It can be seen that the coating microhardness of pure nickel is 307 HV and the microhardness of coating with the content of 2.5 wt% is 511 HV. Thus, it can be seen that the hardness of composite coating is higher than pure Ni coating and the microhardness of coating increases with the increase of Al<sub>2</sub>O<sub>3</sub> content. The more the Al<sub>2</sub>O<sub>3</sub> content, the more obvious the strengthening effect. The increase of coating hardness is due to: (1) the Al<sub>2</sub>O<sub>3</sub>-nanoparticles are distributed in the coating evenly, playing a dispersion-strengthening role in greatly increasing the number of dislocation, twin crystal and various defects in coating; (2) the Al<sub>2</sub>O<sub>3</sub>-nanoparticles restrain the grain growth and result in the compaction of coating texture in the process of deposition.

### 3.4. Bonding strength

Figure 7 shows the tensile fracture of the nanocomposite after bonding strength test. It is obvious that fracture occurs at the junction surface between coating and substrate, where there is supposed to be the weak position on the entire coating.

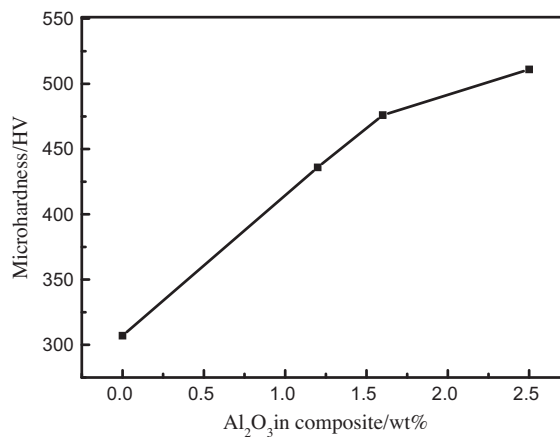


Figure 6. Effect of wt% of Al<sub>2</sub>O<sub>3</sub> in the composite on microhardness.





Figure 7. Cross-sectional morphology of the breaking example.

Test results indicate that, when the specimen thickness reached about 100  $\mu\text{m}$ , the bonding strengths were 8.5, 12.3, and 9.9 MPa, respectively, on the coating of pure nickel, composite with 1.6 wt%  $\text{Al}_2\text{O}_3$  and the one with 2.5wt%  $\text{Al}_2\text{O}_3$ . It reveals that, if  $\text{Al}_2\text{O}_3$  content is relatively low, bonding strength is better than pure nickel, but will get worse along with the increase of the  $\text{Al}_2\text{O}_3$  content. The reason is that the combination between the coating and substrate mainly depends on the bonding of substrate and metal matrix. The nanoparticles embedded in coating can refine grain, which indirectly extends the bonding area between metal matrix and substrate, thus effectively improving the bonding strength. As the amount of  $\text{Al}_2\text{O}_3$  in the coating increases, the interface of metal matrix and substrate correspondingly contains more  $\text{Al}_2\text{O}_3$  particles resulting in smaller effective bonding area. When the effect of decreasing bonding area due to increasing incoming particulates is more significant than that of metal grain refining which help extend bonding surface, the bonding strength begins to gradually decline as the  $\text{Al}_2\text{O}_3$  content increases.

### 3.5. Corrosion behavior

According to the data obtained from the coating static test in 4% HCl solution for 48h, the average corrosion rate of the coating is as shown in Table 2. When the content is low (1.6wt%), the nanoparticles cannot play the dispersion role but reduce the corrosion resistance of coating making it worse than nickel coating. When the content is high (2.5wt%), the nanoparticles will easily produce agglomeration, leading that the structure of composite coating is not compact, the corrosion resistance is bad and relatively lower, but better than pure nickel coating. All this shows that it is important to select appropriate nanocontent to improve the corrosion resistance of coating. The high or low content is bad for its corrosion resistance [10]. Through 48h corrosion test, we found that the surface of pure nickel coating had a lot of corrosion pits and the surface of coating with nano- $\text{Al}_2\text{O}_3$  content of 1.6wt% is smooth and the corrosion pits are not obvious. This further states that the composite coating with a certain content of nano- $\text{Al}_2\text{O}_3$  can really improve the corrosion resistance of the coating.

Table 2. Average corrosion rate of the different composite coatings.

Corrosion rate	The $\text{Al}_2\text{O}_3$ content/wt%			
	0	1.2	1.6	2.5
$\text{g m}^{-2} \text{h}^{-1}$	1.72	1.90	0.70	0.92



#### 4. Conclusions

The nanocomposite coatings with different  $\text{Al}_2\text{O}_3$  content were prepared by jet electrodeposition and the related composition and structure was investigated.

The  $\text{Al}_2\text{O}_3$  content in the composites first increase then decrease with the increase in the concentrations of  $\text{Al}_2\text{O}_3$ , current density as well as jet speed. The maximum wt% of  $\text{Al}_2\text{O}_3$  in the composite is high up to 12.2. The higher the  $\text{Al}_2\text{O}_3$  content, the composite becomes more smooth and impact. The composite coating is face-centered cubic structure and represented a (200) preferential orientation. Microhardness of the coating increase, bonding strength and corrosion resistance of the coatings first increase then decrease with increase of  $\text{Al}_2\text{O}_3$  content in coatings.

#### Acknowledgments

The work described in this paper was supported the National Science Foundation of China (No. 51105162) and Natural Science Foundation of Jiangsu Colleges and Universities (No. 11KJD460003).

#### Reference

- [1] Xue YJ, Zhu D, Zhao F. Electrodeposition and mechanical properties of Ni- $\text{La}_2\text{O}_3$  nanocomposites. *Journal of Materials Science*. 2004;39:4063–6.
- [2] Liu Y, Ren LQ, Yu S, Han ZW. Influence of current density on nano- $\text{Al}_2\text{O}_3/\text{Ni}+\text{Co}$  bionic gradient composite coatings by electrodeposition. *Journal of University of Science and Technology*. 2008;15:633–7.
- [3] Qiao GY, Jing TF, Wang N. High-speed jet electrodeposition and microstructure of nanocrystalline Ni-Co alloys. *Electrochemical Acta*. 2005;16:46–50.
- [4] Xu BS, Wang HD, Dong SY, Jiang B. Fretting wear-resistance of Ni-base electro-brush plating coating reinforced by nano-alumina grains. *Materials Letters*. 2006;60:710–3.
- [5] Dai PQ, Xu WC, Huang QY. Mechanical properties and microstructure of nanocrystalline nickel-carbon nanotube composites produced by electrodeposition. *Materials Science and Engineering: A*. 2008; 483–484:172–4.
- [6] Wu B, Xu BS, Zhang B, Lu YH. Preparation and properties of Ni/nano- $\text{Al}_2\text{O}_3$  composite coatings by automatic brush plating. *Surface and Coatings Technology*. 2007;201:6933–9.
- [7] Wei XY, Dong HS, Lee CH, Jiang K. Determination of young's modulus of electrochemically co-deposited Ni- $\text{Al}_2\text{O}_3$  nanocomposite. *Materials Letters*. 2008;62:1916–8.
- [8] Feng QY, Li TJ, Zhang ZT, Zhang J, Liu M. Preparation of nanostructured Ni/ $\text{Al}_2\text{O}_3$  composite coatings in high magnetic field. *Surface and Coatings Technology*. 2007;14:6247–52.
- [9] Zhou Y, Zhang H, Qian B. Friction and wear properties of the co-deposited Ni-SiC nanocomposite coating. *Applied Surface Science*. 2007;20:8335–9.
- [10] Feng QY, Li TJ, Teng HT, Zhang XL, Liu CS, Jin JZ. Investigation on the corrosion and oxidation resistance of Ni- $\text{Al}_2\text{O}_3$  nano-composite coatings prepared by sediment co-deposition. *Surface and Coatings Technology*. 2008;17:4137–44.